IN-32-CR

118832

p.27

THE OHIO STATE UNIVERSITY

(NASA-CR-182397) BACKSCATTER FROM A PERIODIC ROUGH SURFACE AT NEAR GRAZING INCIDENCE (Ohio State Univ.) 27 p CSCL 20N

N88-15128

Unclas

G3/32 0118832

Backscatter From A Periodic Rough Surface At Near Grazing Incidence

A.K. Dominek and H.T. Shamansky

The Ohio State University

ElectroScience Laboratory

Department of Electrical Engineering
Columbus, Ohio 43212

R.M. Wood
NASA Langley Research Center
Hampton, Virginia 23665

Technical Report No. 716148-24
Grant NSG 1613
October 1987

National Aeronautics and Space Administration
Langley Research Center
Hampton, VA 22217

NOTICES

50272-101

REPORT DOCUMENTATION PAGE

1. REPORT NO.

2.

3. Recipient's Accession No.

4. Title and Subtitle

BACKSCATTER FROM A PERIODIC ROUGH SURFACE AT NEAR GRAZING INCIDENCE

5. Report Date

October 1987

6.

7. Author(s) R.M. Wood, NASA Langley Research Center
A.K. Dominek and H.T. Shamansky, OSU-ElectroScience Laboratory

8. Performing Organization Rept. No.

716148-24

9. Performing Organization Name and Address

The Ohio State University
ElectroScience Laboratory
1320 Kinnear Road
Columbus, Ohio 43212

10. Project/Task/Work Unit No.

11. Contract(C) or Grant(G) No.

(C)

(G) NSG 1613

12. Sponsoring Organization Name and Address

National Aeronautics and Space Administration
Langley Research Center
Hampton, Virginia 22217

13. Type of Report & Period Covered

Technical

14.

15. Supplementary Notes

16. Abstract (Limit: 200 words)

The effect of periodic surface roughness on the radar cross section (RCS) was studied. The surface roughness was formed by a small sinusoidal variation in a planar surface. RCS measurements were obtained for two different sinusoidal variations near grazing incidence for both principal polarizations. Significant grating lobes were observed in the measurements which directly correspond to the roughness characteristics. A physical optics solution was generated and compared to the measurements with reasonable agreement.

17. Document Analysis a. Descriptors

b. Identifiers/Open-Ended Terms

c. COSATI Field/Group

18. Availability Statement

19. Security Class (This Report)

Unclassified

20. Security Class (This Page)

Unclassified

21. No. of Pages

22

22. Price

(See ANSI-Z39.18)

See Instructions on Reverse

OPTIONAL FORM 272 (4-77)
(Formerly NTIS-35)
Department of Commerce

Contents

PRECEDING PAGE BLANK NOT FILMED

List of Figures

Chapter 1

Introduction

Aerodynamic structures are often designed to have "smooth" surface contours. Frequently this "smooth" surface results in a somewhat distorted or rough surface due to the connection points of the outer skin to ribs and bulkheads. The surface is well defined at these connection points but is allowed to vary between them, and the resulting surface is no longer smooth due to a very small oscillatory behaviour.

The surface roughness introduced into the actual structure is undesirable from an electromagnetic scattering view point. The scattered field from an isolated area of the surface is insignificant, yet the periodic nature of the surface roughness due to the regularly spaced bulkheads and ribs compounds the effect of the individually distorted areas. The effect of this periodicity can generate a significant backscattered field at some incidence angle and frequency because the scattered field from each individual perturbation adds constructively.

This report presents measured and calculated results for backscatter

from a rough surface due to a sinusoidal surface variation.

Chapter 2

Rough Surface Definition

A simple sinusoidal surface variation over a planar surface was chosen to demonstrate the scattering from a periodic surface. Sinusoidal surface variations were machined into two aluminium plates, each .375 inch thick. The planar extent of this roughness was 11 by 36 inches with a 1 inch period and peak to peak variation of .01 and .03 inches for the two plates respectively. Figure 2.1 is a picture of one plate illustrating the geometry.

ORIGINAL PAGE
BLACK AND WHITE PHOTOGRAPH

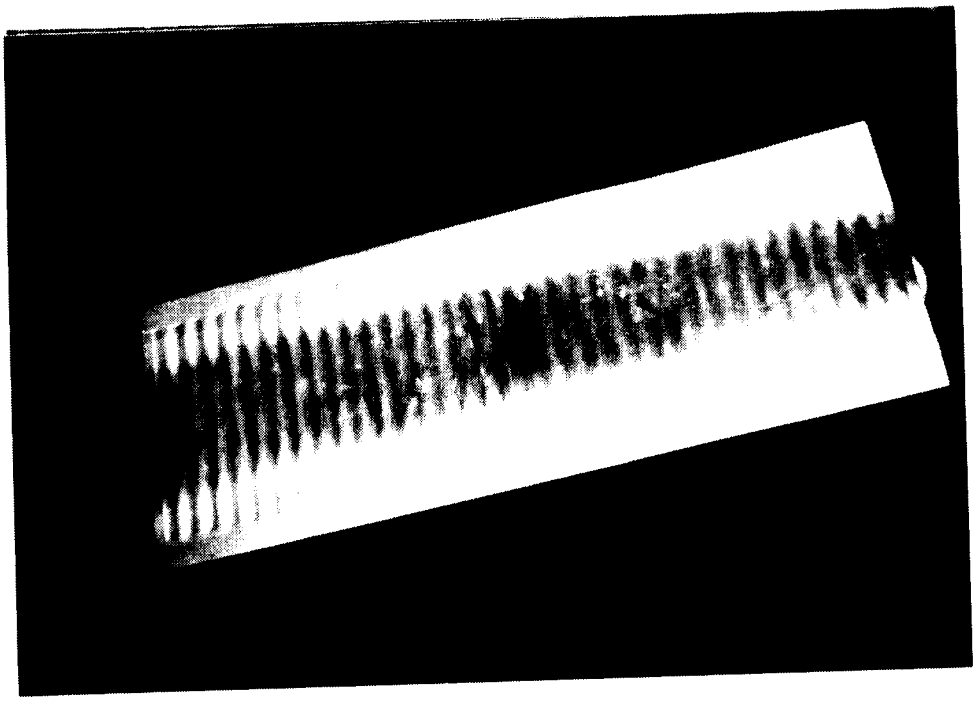

Figure 2.1: Planar metal surface with a sinusoidal surface variation.

Chapter 3

Measurements

Swept frequency backscatter RCS (radar cross section) measurements were taken for the two plates with both principal polarizations. The plates were aligned with the incident field normal to the translation of the sinusoidal variation. Incidence angles of 10°, 20° and 30° from grazing were measured. Each measured spectrum was numerically transformed into the time domain using an FFT. The time reference for time equalling zero for the transient signatures is located at the center of the plates. Figures 3.1 through 3.3 are the E-plane measurements for the plate with surface variations of .01 inches at grazing angles of 10°, 20° and 30°, respectively. Figures 3.4 through 3.6 are the H-plane measurements for the plate with surface variations of .01 inches at grazing angles of 10°, 20° and 30°, respectively. Figures 3.7 through 3.9 are the E-plane measurements for the plate with surface variations of .03 inches at grazing angles of 10°, 20° and 30°, respectively.

Figures 3.10 through 3.12 are the H-plane measurements for the plate with surface variations of .03 inches at grazing angles of 10°, 20° and 30°, respectively.

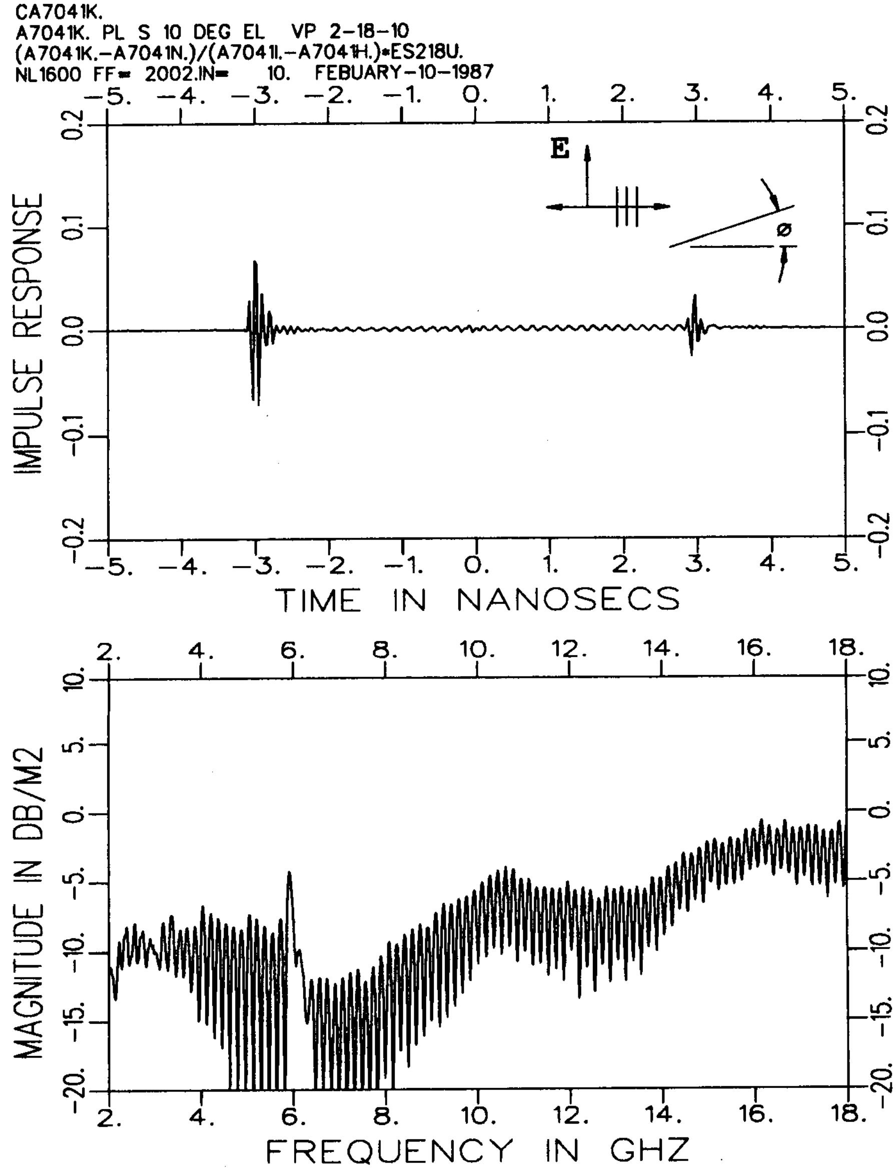

Figure 3.1: E-plane RCS response for sinusoidal surface variation of .01 inches at 10 degrees grazing incidence.

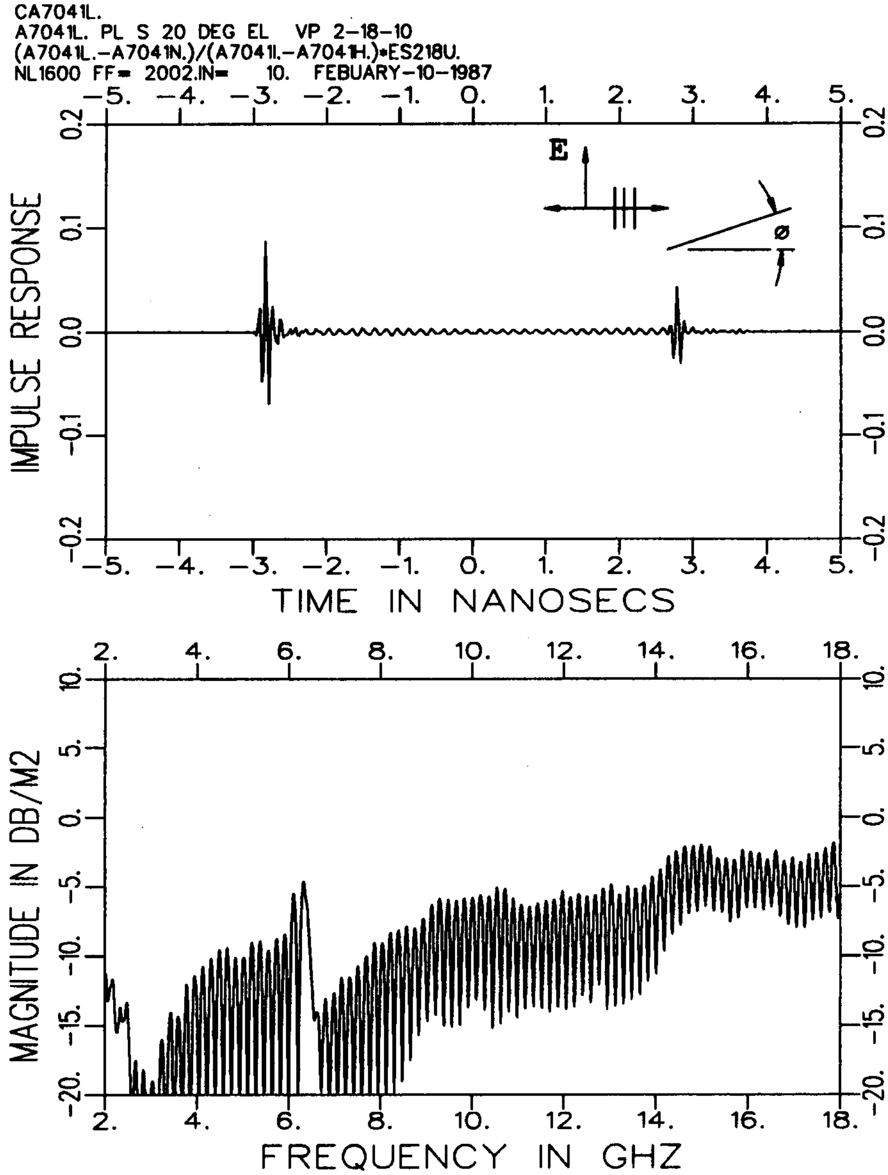

Figure 3.2: E-plane RCS response for sinusoidal surface variation of .01 inches at 20 degrees grazing incidence.

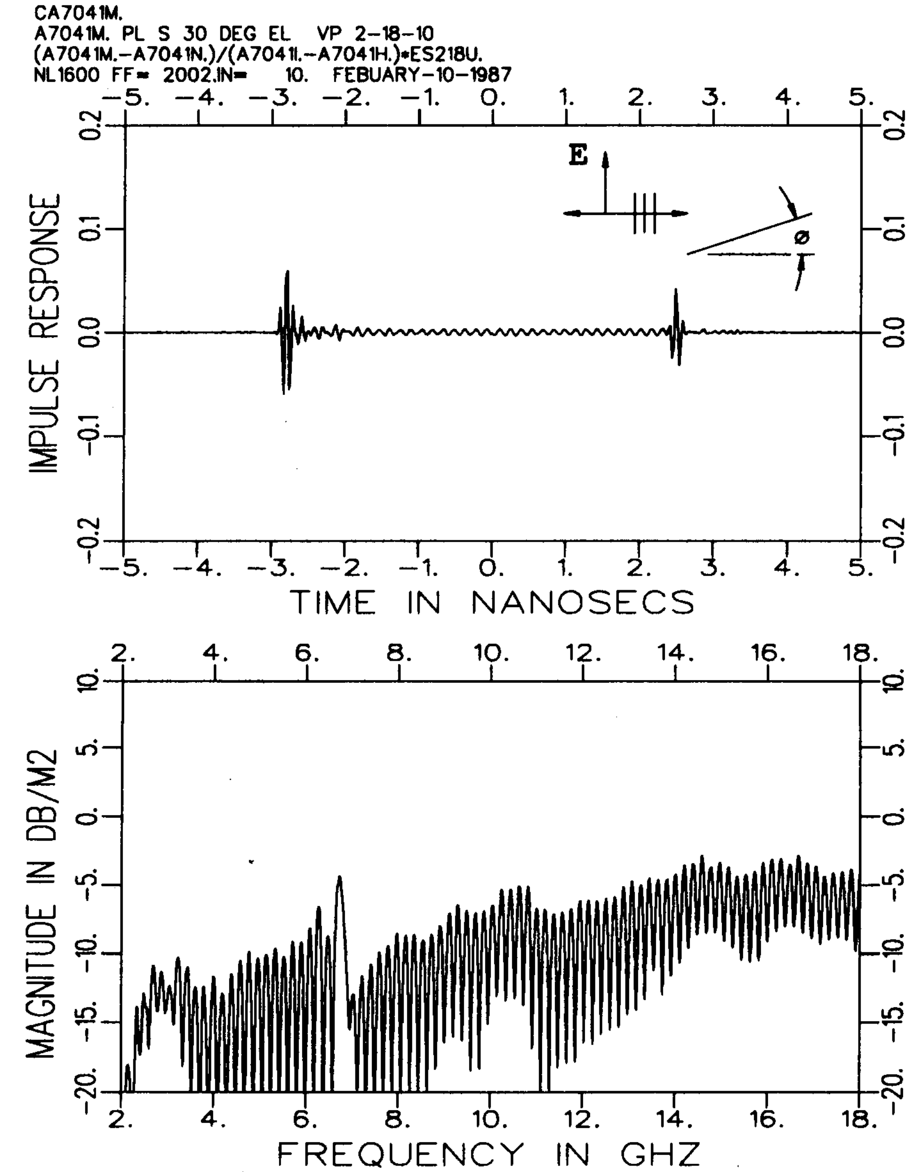

Figure 3.3: E-plane RCS response for sinusoidal surface variation of .01 inches at 30 degrees grazing incidence.

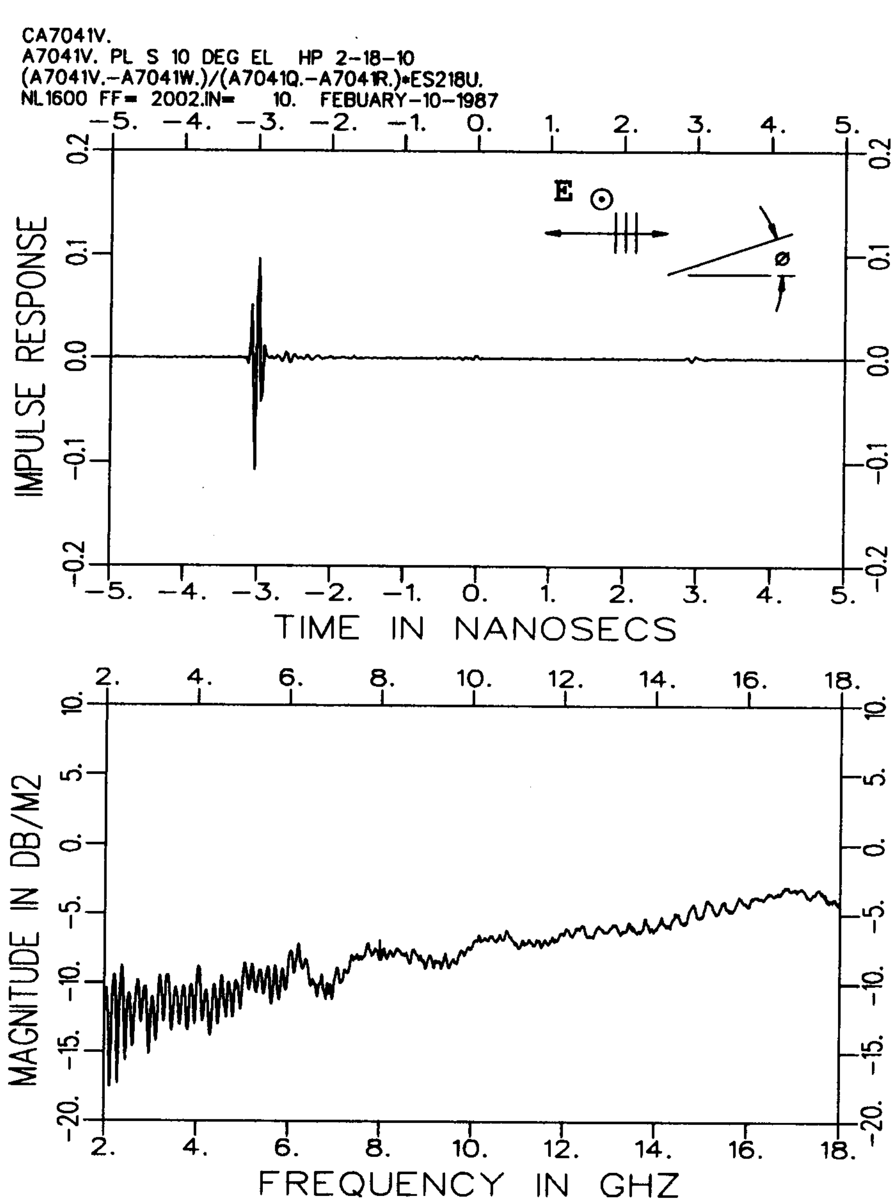

Figure 3.4: H-plane RCS response for sinusoidal surface variation of .01 inches at 10 degrees grazing incidence.

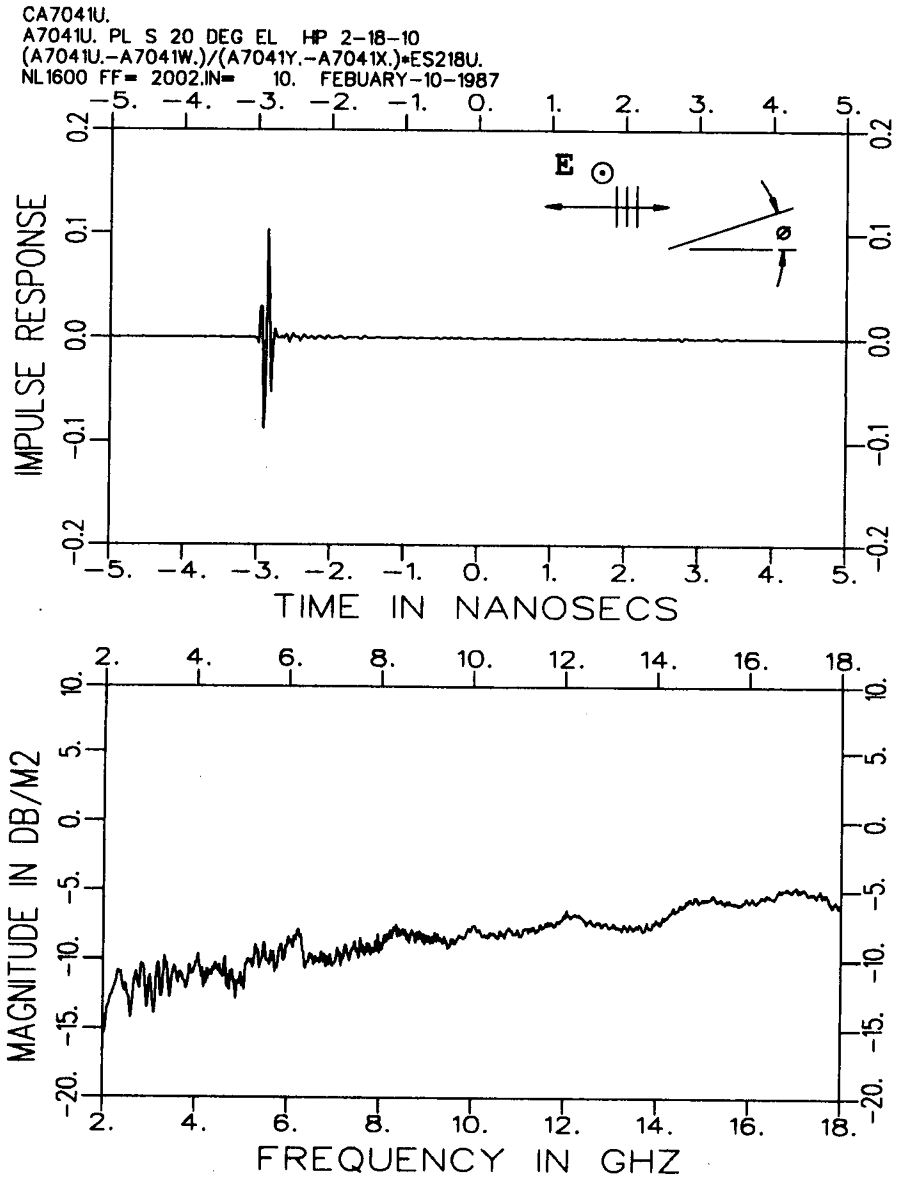

Figure 3.5: H-plane RCS response for sinusoidal surface variation of .01 inches at 20 degrees grazing incidence.

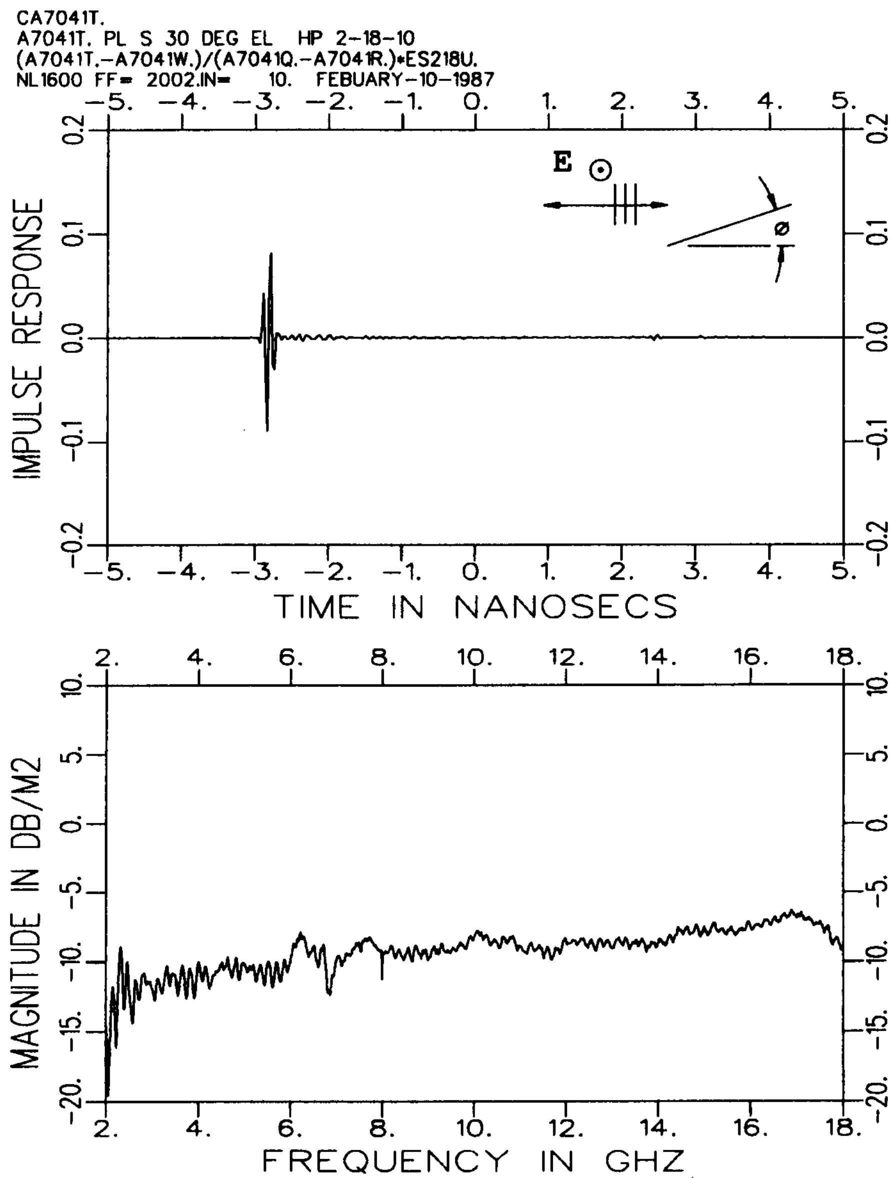

Figure 3.6: H-plane RCS response for sinusoidal surface variation of .01 inches at 30 degrees grazing incidence.

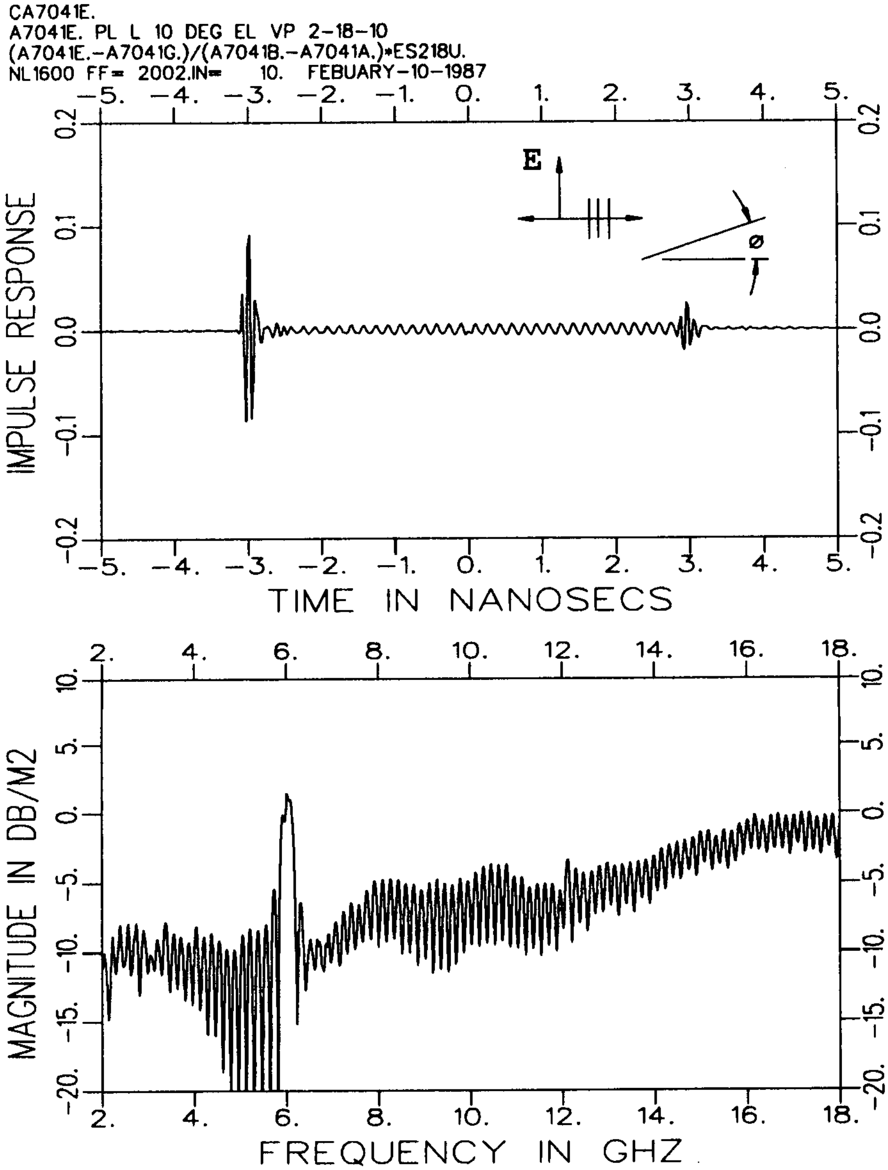

Figure 3.7: E-plane RCS response for sinusoidal surface variation of .03 inches at 10 degrees grazing incidence.

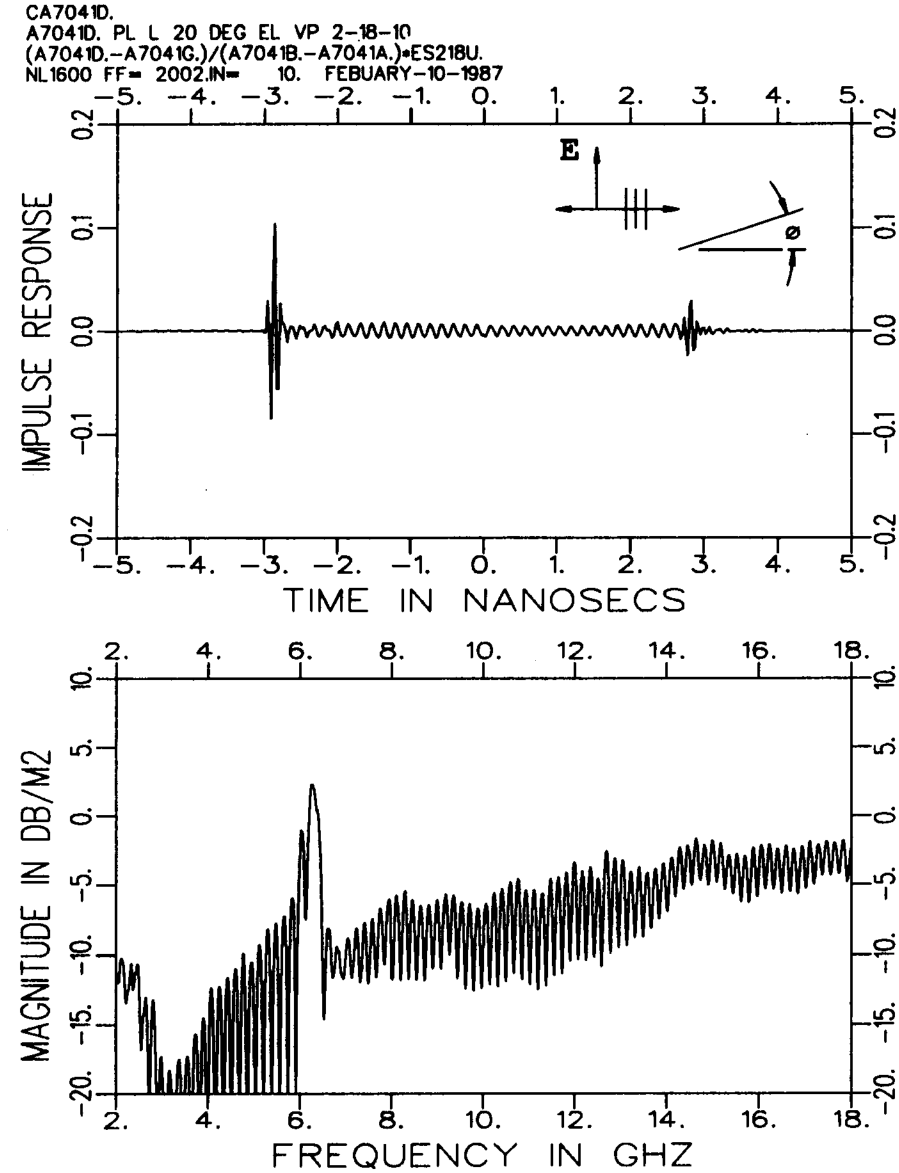

Figure 3.8: E-plane RCS response for sinusoidal surface variation of .03 inches at 20 degrees grazing incidence.

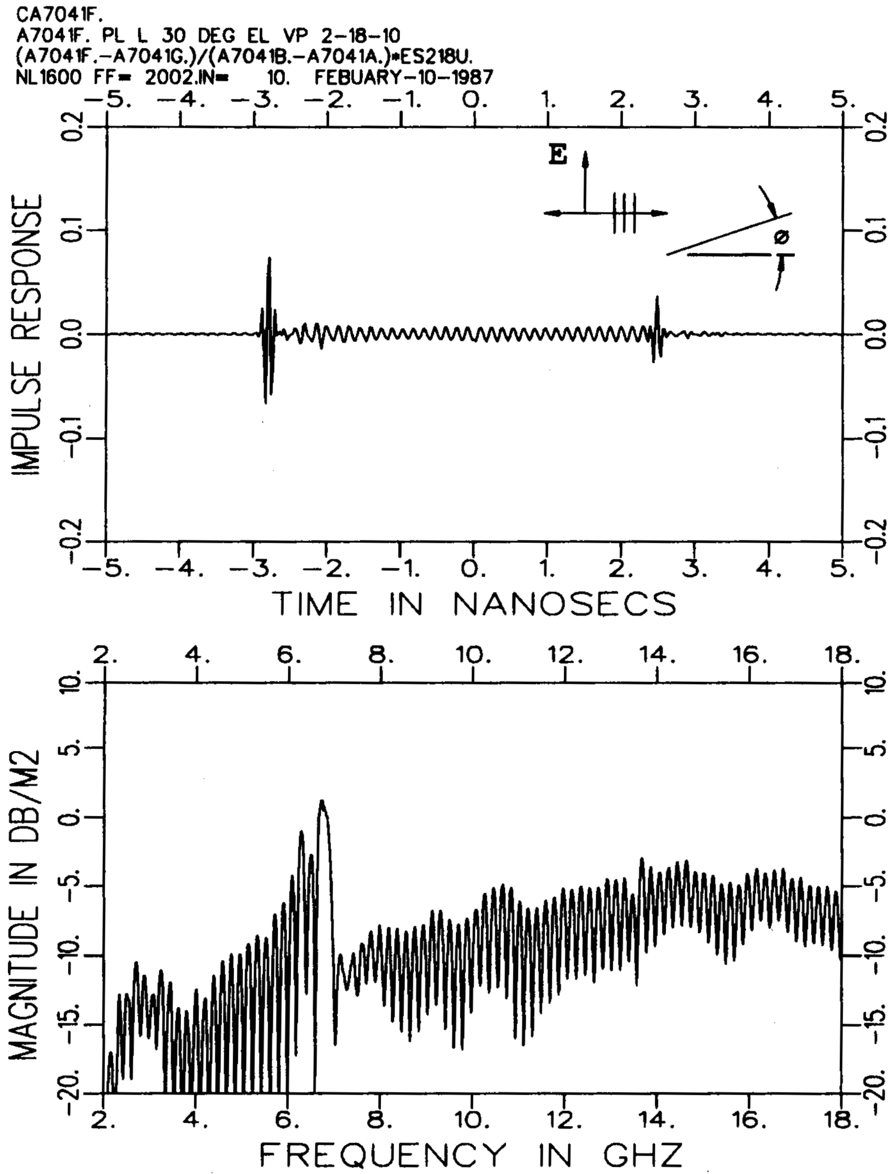

Figure 3.9: E-plane RCS response for sinusoidal surface variation of .03 inches at 30 degrees grazing incidence.

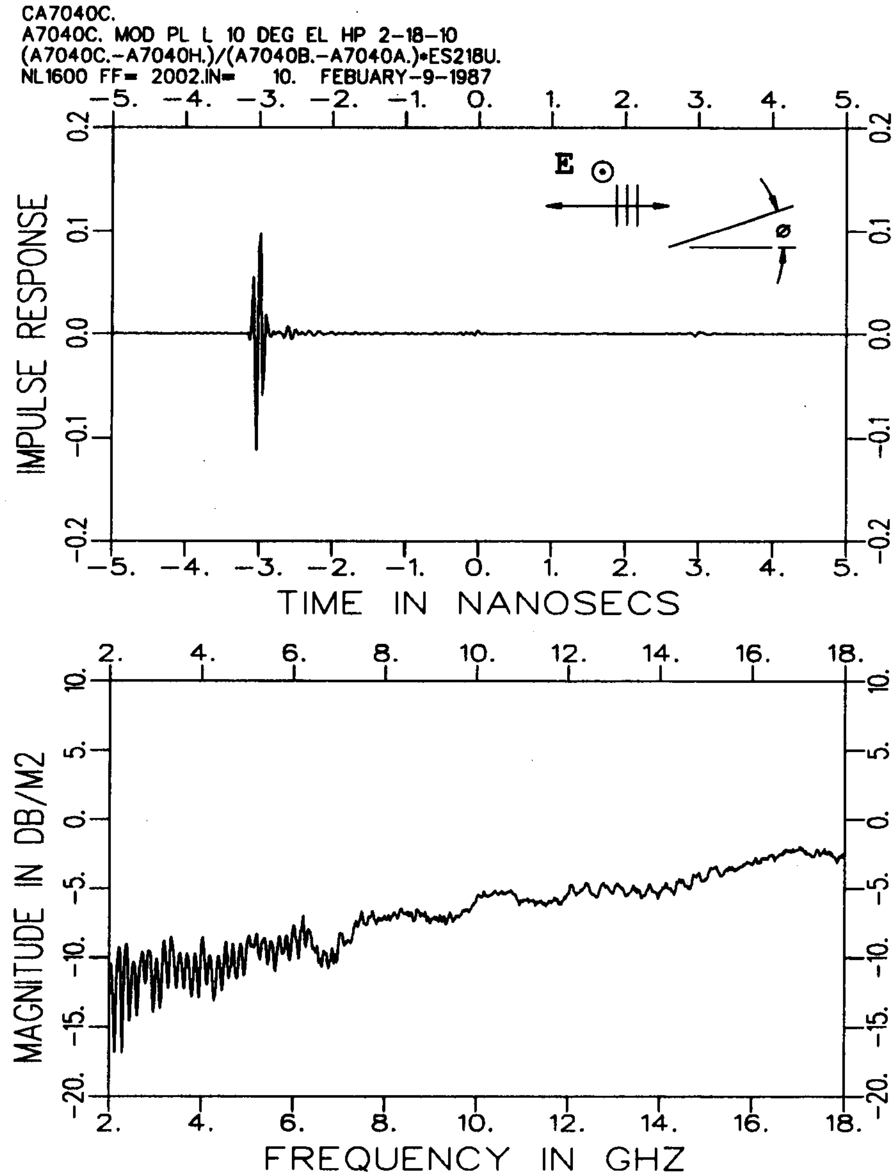

Figure 3.10: H-plane RCS response for sinusoidal surface variation of .03 inches at 10 degrees grazing incidence.

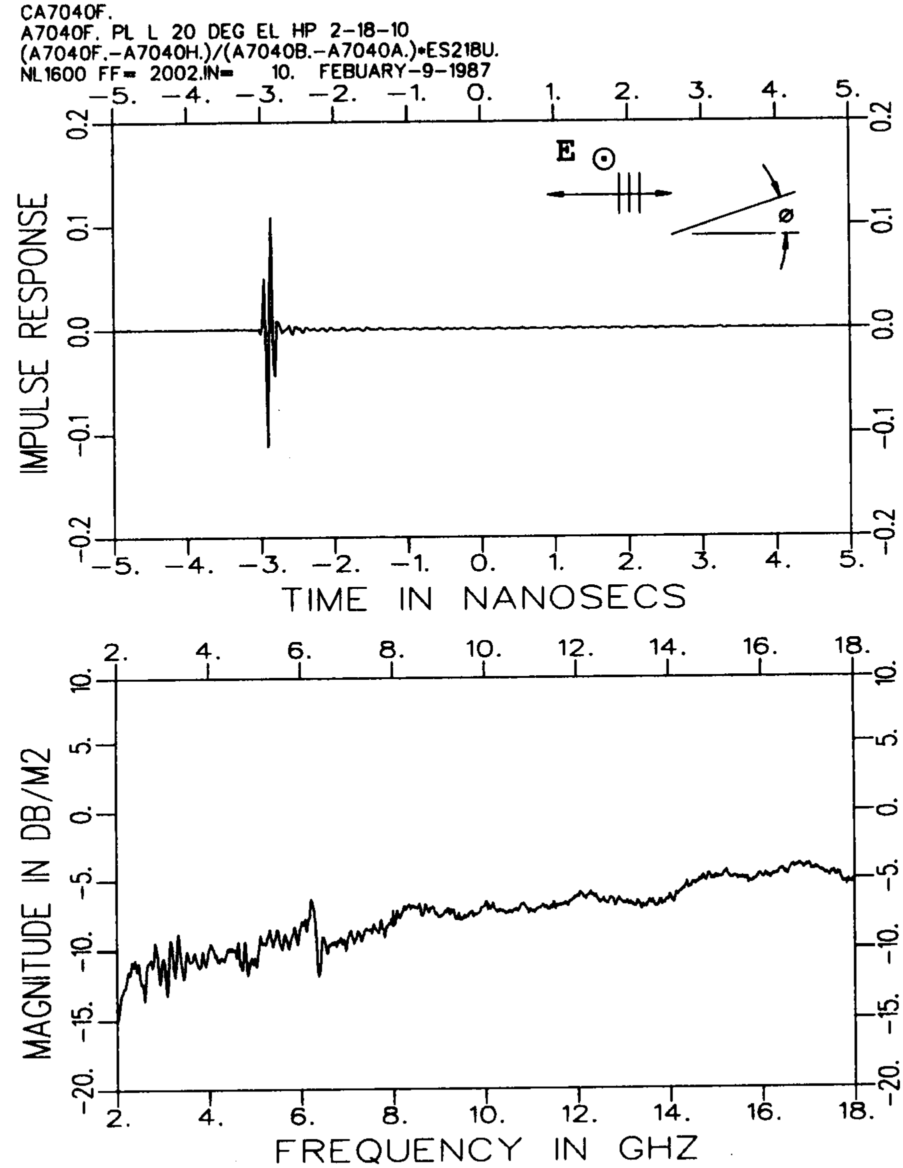

Figure 3.11: H-plane RCS response for sinusoidal surface variation of .03 inches at 20 degrees grazing incidence.

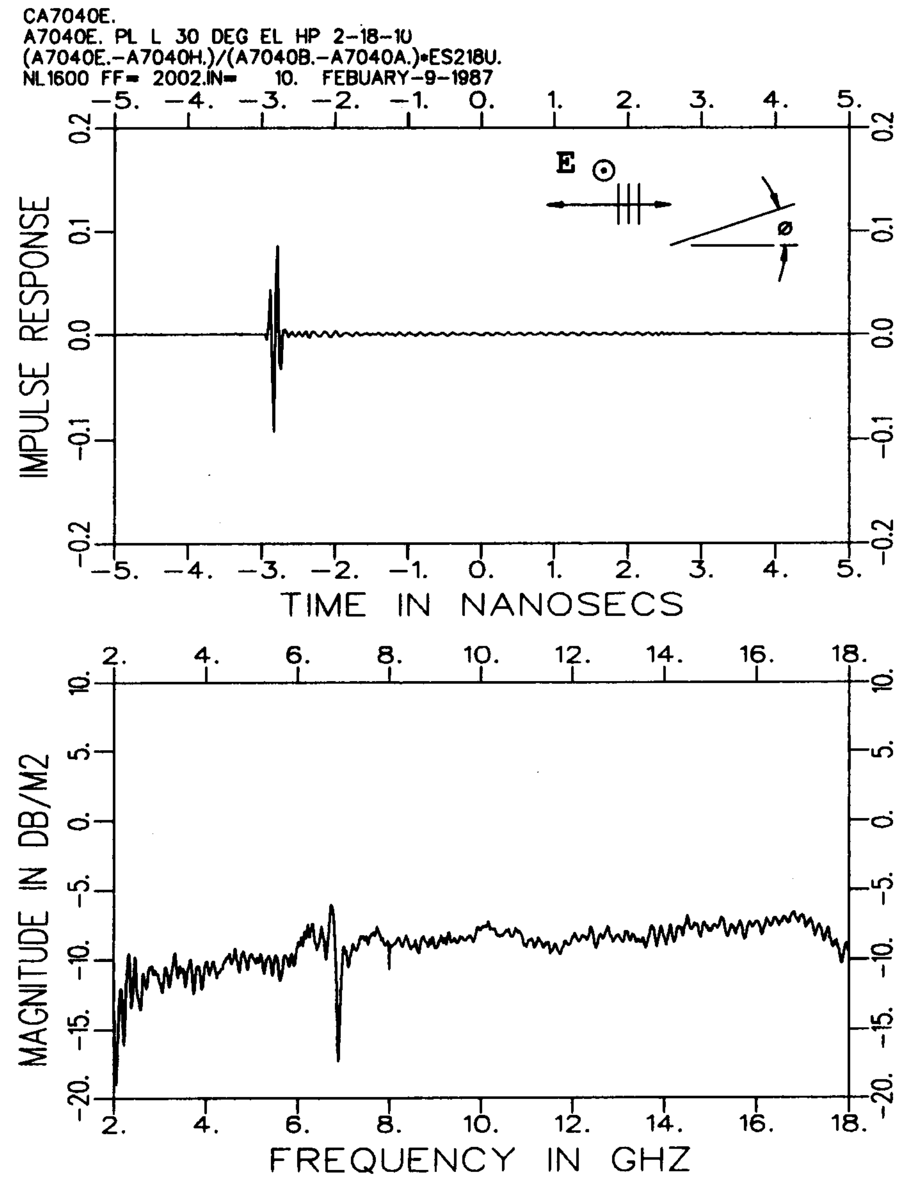

Figure 3.12: H-plane RCS response for sinusoidal surface variation of .03 inches at 30 degrees grazing incidence.

Note the similarity of the features on the plots. The spectra have a rapid variation due to the interaction of the leading and trailing edges which is shown on transient signatures. The important feature is the lobe occurring at roughly 6 GHz. The surface roughness induces a scattering which is additive in nature, thereby causing the grating lobe. This feature is portrayed by the oscillatory trace between the leading and trailing edges in the time domain plot. The frequency position of this lobe is determined when corresponding surface points are one-half lambda apart and is given by

$$f_l = \frac{c}{2d_p \cos\theta} \tag{3.1}$$

were c is the speed of light, d_p is the period of variation and θ is the angle of grazing. Also notice that the magnitude of the lobe is rather insensitive to the angle of incidence.

The most critical polarization for grating lobe scattering is when the plane containing the electric incident field is normal to the roughness as demonstrated in the measurements. When the electric field is parallel to the surface, the image field tends to cancel the incident field and thereby does not produce a strong scattered field.

Another measurement was performed to highlight the scattering from this periodic surface. Resistive edge card was used to treat the leading and trailing edges of the plate with the .03 inch variation. Figure 3.13 is the scattered field response for this treated plate at 10° grazing incidence with E-plane polarization. Note the appearance of the second grating lobe around 12 GHz. Overlaid on this measurement is the physical optics (PO) calculation of the scattered field due to surface roughness. The agreement is reasonable between the measurement and calculation considering that PO is generally unreliable for grazing angles of incidence.

Figure 3.14 contains a family of curves based upon physical optics for the RCS due to sinusoidal surface roughness. The calculations are for a surface 11 by 36 inches with 36 periods with each period being 1 inch. The curves are for grazing incidence angles of 10°, 20° and 30°. The amplitude of the sinusoidal roughness was varied between .001 and .015 inches. The incident field frequency was controlled such that the first grating lobe appeared at the desired incident angle.

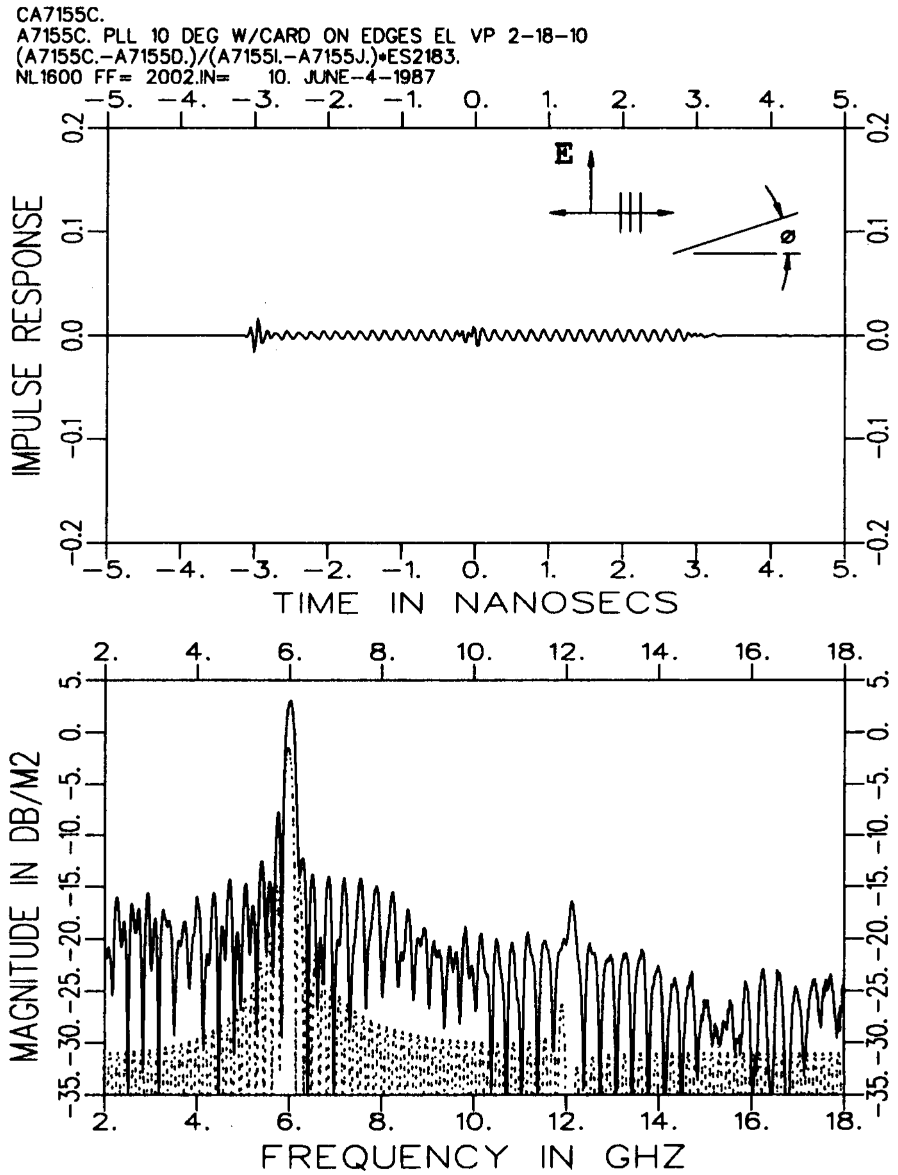

Figure 3.13: E-plane RCS response for sinusoidal surface variation of .03 inches at 10 degrees grazing incidence. Solid-measured with edge treatment on plate. Dashed-physical optics calculation.

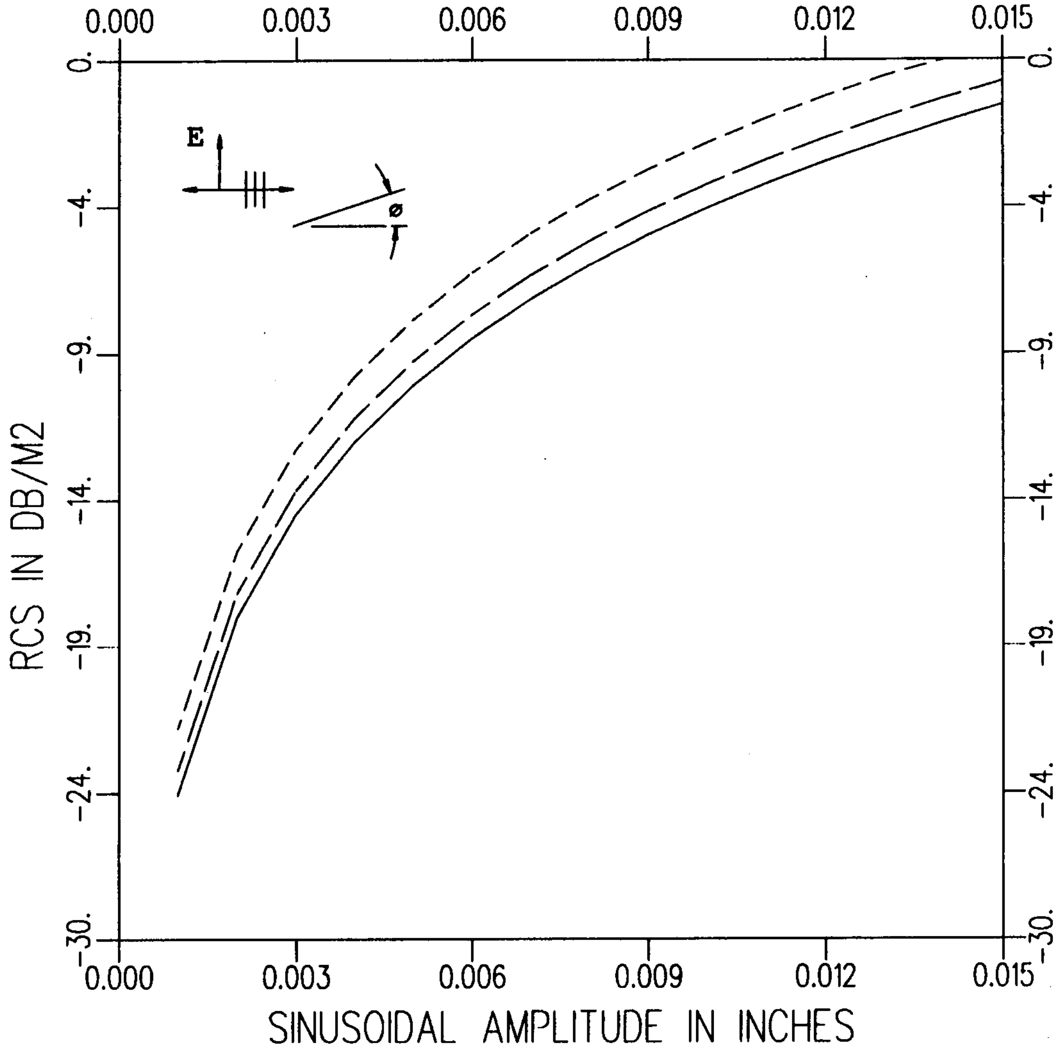

Figure 3.14: RCS for sinusoidal surface roughness with 36 periods, 1 inch periods. Incident field frequency is adjusted so the first grating lobe appears at the incident angle. Angle of incidence: 10° solid, 20° long dash, 30° short dash.

Chapter 4

Conclusions

The scattering from periodic surface roughness for backscatter can be significant for low cross section vehicles at a given frequency and observation angle. The greatest scattering can be observed when the magnetic field is parallel to the surface. When the electric field is parallel to the surface, the image field tends to cancel the incident field and thereby does not produce a strong scattered field. The magnitude of the grating lobes is sensitive only slightly to the angle of incidence but much more to the roughness of the surface. The grating lobe effect can be controlled by destroying the periodicity of the roughness.